J Electroceram (2009) 22:82–86
DOI 10.1007/s10832-007-9393-y

Structural and electrical properties of Sb-doped p-type ZnO thin films fabricated by RF magnetron sputtering

Dong Hun Kim · Nam Gyu Cho · Kyoung Sun Kim · Seungho Han · Ho Gi Kim

Received: 15 March 2007 / Accepted: 11 December 2007 / Published online: 28 June 2008

Abstract We investigated the Sb-doping effects on ZnO thin film using RF (radio frequency) magnetron sputtering and RTA (rapid thermal annealing). The structural and electrical properties of the thin films were measured by X-ray diffraction, SEM (scanning electron microscope), and Hall effect measurement. Thin films were deposited at a high temperature of 800°C in order to improve the crystal quality and were annealed for a short time of only 3 min. The structural properties of undoped and Sb-doped films were considerably improved by increasing oxygen content in the Ar-O_2 gas mixture. Sb-doping also significantly decreased the electron concentration, making the films p-type. However, the crystallinity and surface roughness of the films degraded and the mobility decreased while increasing Sb-doping content, likely as a result of the formation of smaller grain size. From this study, we observed the transition to the p-type behavior at 1.5 at.% of Sb. The thin film deposited with this doping level showed a hole concentration of 4.412×10^{17} cm^{-3} and thus is considered applicable to p-type ZnO thin film.

Keywords p-type ZnO · Sb-doping · Sputtering · Hall measurement

1 Introduction

ZnO pertains to the wide band gap semiconductor for optoelectronics applications because of its large direct wide band gap (E_g~3.3 eV at 300 K) and large exciton binding energy (~60 meV, cf. ~25 meV for GaN) [1–3]. In order to build an effective light emitting diode (LED) incorporating ZnO, both high quality n-type and p-type ZnO are absolutely needed. It is well known that undoped ZnO thin films have n-type properties due to intrinsic defects and it is very difficult to achieve a p-type behavior for a ZnO layer because of the "self-compensation" resulting from spontaneously generated donor defects such as oxygen vacancies or zinc interstitials [4] or hydrogen impurities from the crystal growth environment [5]. Low solubility of the dopant in the ZnO matrix is another obstacle to p-type ZnO [6]. In order to synthesis p-type ZnO, group I elements (Li, Na, and K) for Zn sites or group V elements (N, P, As, and Sb) for oxygen sites can be used as substitutional dopants. The doping efficiency of I element is poor because of their potential occupancy of interstitial sites origination from their small ionic radii [7]. Many researchers tried to obtain p-type ZnO with group V elements such as N [8–9], P [10–11], and As [12]. However, good device performances are not demonstrated yet. Recently, on the basis of first principle calculation, Limpijumnong's group predicted that element Sb, could be introduced shallow acceptor level in ZnO [13].

Following this approach, we deposited Sb-doped ZnO thin films at a high temperature to fabricate high quality p-type epitaxial layer using RF magnetron sputtering. Sb-doping effects on the structural and electrical properties of the fabricated film were also investigated.

2 Experimental details

A mixture of Sb_2O_3 (purity, 99.99%) and ZnO (purity, 99.9%) powders with the Sb-doping content of 0, 1, 3, 5,

D. H. Kim (✉) · N. G. Cho · K. S. Kim · S. Han · H. G. Kim
Department of Materials Science and Engineering, Korea Advanced Institute of Science and Technology,
373-1 Guseong-dong, Yuseong-Gu,
Daejeon 305-701, Republic of Korea
e-mail: rogercopy153@kaist.ac.kr

and 10 at.% were wet-ball milled for 24 h. After drying, the mixture was calcined at 1200°C for 3 h and ball milled again for 24 h. Then dried mixture was cold isostatic pressed at 100 MPa to form the disc shaped target. Sintering was conducted at 1400°C under air atmosphere for 5 h with a heating rate of 5°C/min in box furnace.

Sintered targets were sputtered at 80 W RF power with a mixed gas of oxygen and argon with a ratio of 5:5 to 1:9. The chamber was evacuated by a turbo molecular pump to a base pressure of low 10^{-6} Torr then set to a constant pressure of 10 mTorr. A thermocouple controlled halogen lamp substrate heater was used to control the substrate temperature. During the deposition, sapphire substrates were maintained at 800°C then cooled to room temperature in vacuum. Deposited films were isothermally annealed at RTA for 3 min in oxygen atmosphere with heating rate of 200°C/min. The film thickness was measured by SEM (Scanning Electron Microscopy: Philips XL30SFEG) and experimental conditions were used to deposit 100 nm-thick films because X-ray diffraction and electrical analysis are sensitive to film thickness.

XRD (X-ray Diffraction: Rigaku, D/MAX-RC, λ= 1.5406 Å) analysis was employed to identify the crystalline quality and FWHM (Full width at half maximum) of ZnO (0002) diffraction peaks were produced from θ-rocking curve. Grain size was calculated by Scherrer formula using FWHM value. The carrier concentration, mobility and resisitivity were determined from Hall effect measurement with the van der Pauw method and melted indium dots on the film surface were used for electrical contacts.

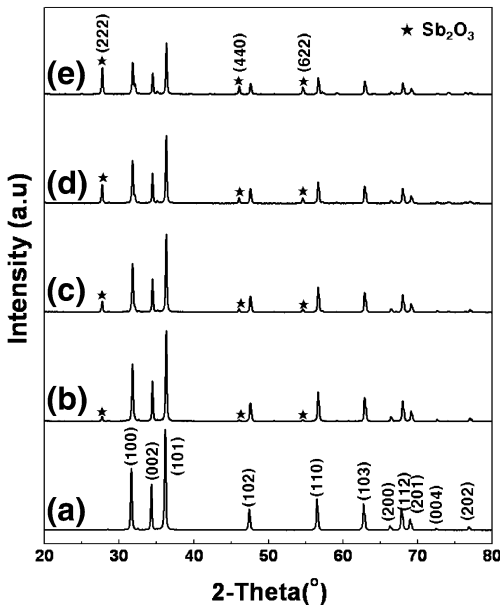

Fig. 1 XRD patterns of Sb_2O_3 mixed ZnO powder before calcination. (**a**) Undoped, (**b**) 1, (**c**) 3, (**d**) 5, and (**e**) 10 at.% Sb-doped ZnO

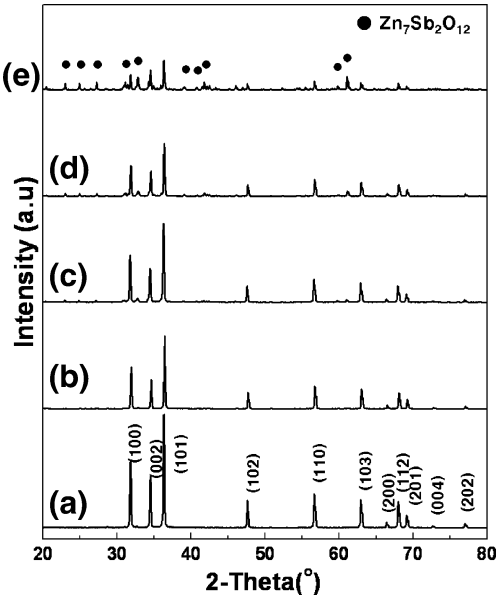

Fig. 2 XRD patterns of Sb-doped ZnO powder after calcination at 1200°C for 3 h. (**a**) Undoped, (**b**) 1, (**c**) 3, (**d**) 5, and (**e**) 10 at.% Sb-doped ZnO

3 Results and discussion

Figure 1 shows the XRD patterns obtained in accordance with the addition of Sb_2O_3 powder after ball milling. Sb_2O_3 powders are distributed randomly with an unreacted state in ZnO matrix because the mixtures are only physically mixed. Consequently Sb_2O_3 peaks are observed, as indicated in Fig. 1(b), (c), (d), and (e). As the amount of added Sb_2O_3 is increased, the intensity of the Sb_2O_3 peaks increases while that of ZnO decreases. In order to substitute Sb dopants into the Zn sites, the mixtures were calcined at 1200°C for 3 h under air atmosphere. As shown in Fig. 2, above 3 at.% [Fig. 2 (c), (d) and (e)], new secondary phase XRD peak of $Zn_7Sb_2O_{12}$ appeared whereas undoped ZnO [Fig. 2(a)] showed only ZnO peaks. From this analysis, we concluded that the solubility limit of Sb to ZnO is 3 at.%.

Figure 3 shows SEM images of 1.0 at.% Sb-doped ZnO thin films deposited at various Ar/O_2 ratios. As the oxygen content in the gas mixture increased, the surface shows enhanced morphology leading to a smooth, flat film morphology of the ZnO thin film. It is supposed that the low deposition rate of ZnO thin films deposited at higher oxygen partial pressure plays a major role in improving the crystallinity as it provides the particles arriving at the substrate sufficient time to diffuse. Undoped, 0.3, and 1.5 at.% Sb-doped ZnO films showed similar trends (not shown here). Rough surface is very harmful to the interfacial, electrical, and cyclic properties of a LED device by acting as a scattering center for electrons of holes. Therefore, we deposited the ZnO thin films under an oxygen rich atmosphere and investigated the structural and

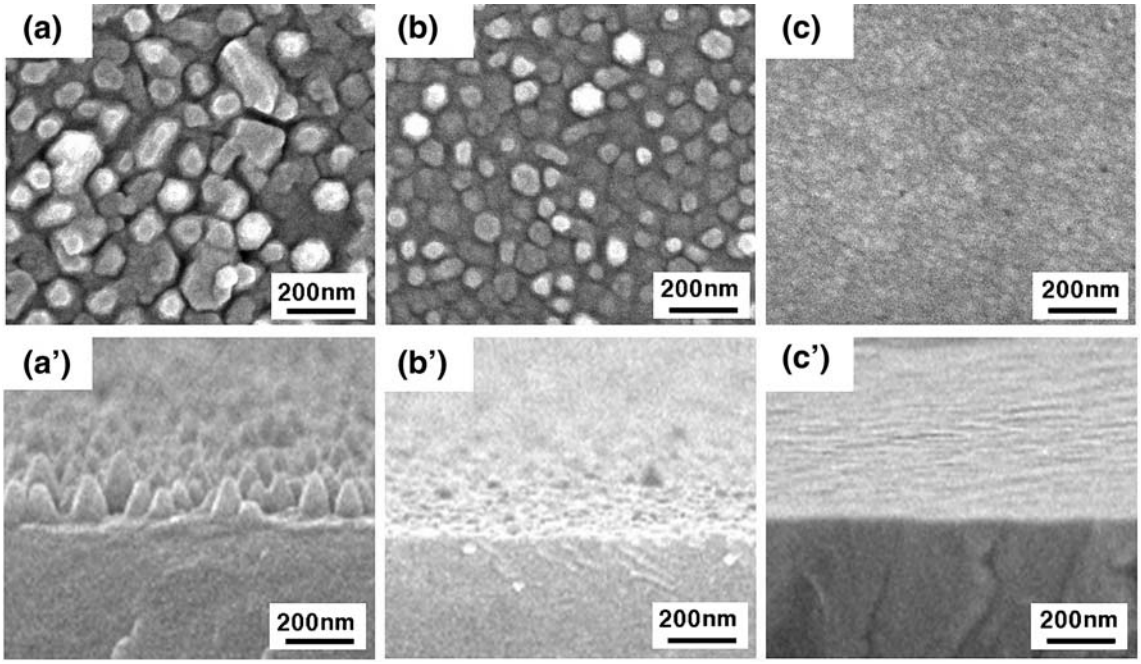

Fig. 3 Surface and cross section images of 1 at.% Sb-doped ZnO thin films grown under various Ar/O_2 gas mixture ratio (**a**), (**a**') 5:5, (**b**), (**b**') 3:7, and (**c**), (**c**') 1:9

electrical properties of ZnO thin films as a function of Sb doping content and annealing atmosphere.

Figure 4 shows the XRD patterns of the Sb-doped ZnO films grown at a substrate temperature of 800°C with an Ar/O_2 gas ratio of 1:9. The maximum of the ZnO (0002) diffraction was observed at 34.35°, 34.31°, 34.29°, and 34.29° for pure, 0.3, 1.0, and 1.5 at.% Sb-doped ZnO films, respectively. The intensity of the ZnO (0002) diffraction peaks decrease while increasing Sb doping. This indicates a degradation of the crystallinity originating form the incorporation of Sb atoms. Using XRD data and the Bragg's equation, the crystal lattice constants of the c axis of the ZnO thin films are 5.215, 5.221, 5.224, and 5.224 Å, for Sb content of 0, 0.3, 1.0, and 1.5 at.% respectively. This can be attributed to a lattice expansion due to large ionic radius of Sb (1.40 Å) compare to that of the oxygen ions (0.73 Å).

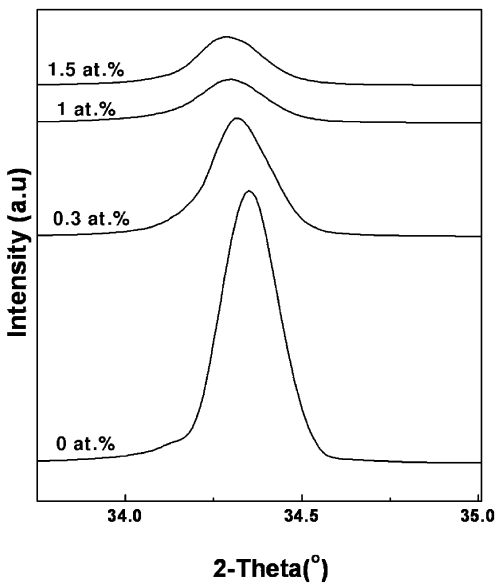

Fig. 4 XRD patterns of Sb-doped ZnO thin films deposited at 800°C and Ar/O_2 gas mixture ratio of 1:9 as a function of Sb-doping content

For further details of doping effects on the structural properties of the ZnO film, we investigated the full width at half maximum (FWHM) values of the θ-rocking curves of Sb-doped ZnO (0002) peaks. In Fig. 5(a) it can be observed that the FWHM value of the Sb-doped ZnO thin films which annealed at 850°C in O_2 ambient for 3 min increases as the Sb doping content increases. This indicates that the Sb doping induces a decrease of the mean crystallite. Also, the grain size was estimated using the Scherrer formula [14] [see also Fig. 5(b)].

$$d = \frac{0.9\lambda}{B \cdot \cos\theta}$$

where d, λ, θ, and B are the mean grain size, the X-ray wavelength (1.54 Å), the Bragg diffraction angle, and FWHM, respectively. The decrease of grain size correlates with a large developed surface of grain boundaries, thus leading to a larger scattering effect, which in turn disturbs the carrier mobility. Therefore, a resistivity enhancement is expected from the Sb doping.

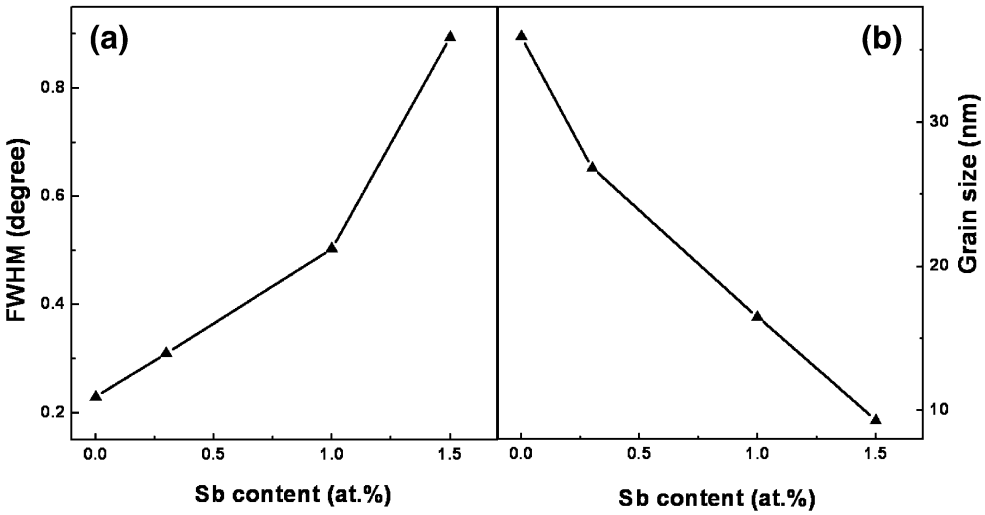

Fig. 5 Variation in the FWHM of the XRD θ-rocking curves of ZnO (0002) diffraction peaks and grain size as a function of Sb-doping content

The electrical properties of Sb-doped ZnO films were assessed on the basis of Hall effect measurements. Figure 6 shows the carrier concentration and resistivity of 1.0 at.% Sb-doped ZnO thin films as a function of oxygen ambient during annealing process. Sb doping on ZnO was predicted to substitute a ZnO site and form a Sb_{Zn}–$2V_{Zn}$ complex compensating the native donor from oxygen vacancies [13].

$$Sb_{Zn}^{3+} + V_{Zn}^{2-} \rightarrow (Sb_{Zn} - V_{Zn})^{+}$$

However, all the films exhibit n-type behavior with an electron concentration of ~10^{17}/cm^3 because the number of electrons from native defects overwhelms the number of holes from Sb dopants. On the other hand, the electron concentration of the 1.0 at.% Sb-doped ZnO films decreased abruptly after annealing in air. And it is thought that the electron concentration would decrease continuously. Against our expectation, the electron concentration decrease at higher oxygen pressure. The cause can be understood by segregation of Sb dopants at the interstitial sites or grain boundary under oxygen rich ambient. From the result of the oxygen ambient effect on carrier concentration, we determined that the optimal oxygen pressure in RTA (rapid thermal annealing) is 2 Torr. As shown in right axis of Fig. 6, the resitivity marked maximum value at minimum point of carrier concentration. (Note that minus means that the numbers of electrons are much lager than that of holes.) The cause is most likely due to the formation of an acceptor level by Sb substitution on oxygen site. The excess electrons from native donors may be compensated by this acceptor, making a reduction of carrier concentration. Therefore, the resistivity of Sb-doped ZnO thin film shows maximum vales at minimum point of carrier concentration.

In other to investigate the correlation between doping content and carrier concentration or resistivity, we deposited at various Sb doping content. All films were annealed at 850°C in O_2 ambient of 2 Torr for 3 min in RTA. Figure 7 shows the carrier concentration and resistivity of

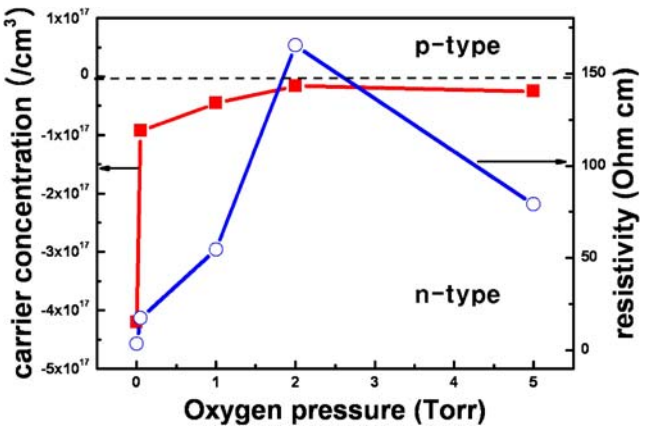

Fig. 6 Dependence of the carrier concentration and resistivity of 1.0 at.% Sb-doped ZnO thin films on the pressure of oxygen ambient in the annealing at 850°C

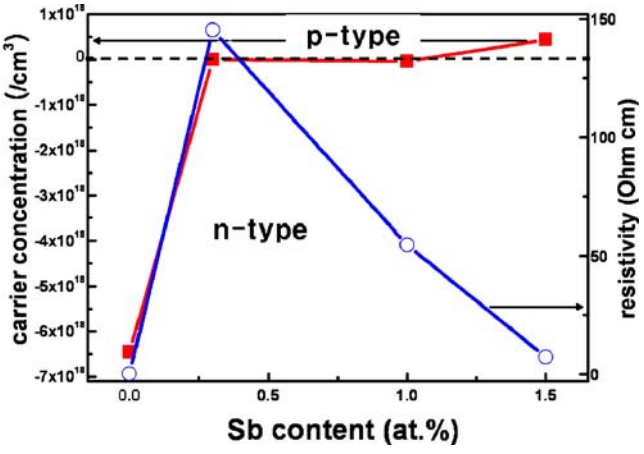

Fig. 7 Carrier concentration and resistivity of undoped and Sb-doped ZnO thin films deposited at 800°C and annealed at 850°C in O_2 ambient for 3 min with respect to Sb doping content

undoped and Sb-doped ZnO thin films as a function of Sb doping content. Undoped ZnO shows n-type property with quite a few of electrons and the number of electron decrease with increasing Sb doping content due to ionization of Sb dopants replaced at oxygen sites. Electron concentration decreases from 4.555×10^{16} cm^{-3} at 0.3 at.% Sb doping content to 5.496×10^{15} cm^{-3} with Sb doping level of 1.0 at.%. At 1.5 at.% Sb-doped ZnO thin film, the number of holes exceed that of electrons and this film shows p-type conduction with a hole concentration of 4.412×10^{17} cm^{-3}. Electrical resistivity increases abruptly from 0.236 Ω cm to 145.4 Ω cm at 0.3 at.% Sb doping content because electron concentration decreases by compensation of excess electrons. As Sb doping contents increase, the resistivity of the Sb-doped ZnO thin films decreases because the excess holes over the number of electrons act as carrier. However, as shown in Fig. 5, at 1.5 at.% Sb-doped ZnO thin film, the grain size becomes smaller and the developed surface of the grain boundaries increased. Consequently, carrier movement is disturbed by grain boundary scattering. Therefore, to deposit a stable and effective p-type ZnO film we must consider higher doping level and the structural epitaxial configurations.

4 Conclusions

We have shown that the Sb-doping strongly influences the structural and electrical properties of ZnO films grown by RF magnetron sputtering on a sapphire substrate. In an effort to fabricate high quality Sb-doped ZnO thin films, we sputtered at high temperature and under oxygen rich ambient. It was found that ZnO thin films became denser and smoother with increasing oxygen content in the sputtering gas. With increasing Sb-doping content, the grain size became small and the surface became rough owing to the larger ionic radius of Sb relative to that of oxygen. Sb doping in ZnO thin films leads to decreased electron concentration and at Sb doping level of 1.5 at.%, the number of holes are more than that of electrons reflecting p-type ZnO. These experimental results indicate that the Sb should be an excellent candidate for p-type ZnO fabrication supporting the achievement of Limpijumnong's group [13].

References

1. D.C. Look, Recent advances in ZnO materials and devices. Mater. Sci. Eng. **B80**, 381 (2001)
2. S.J. Pearton, D.P. Norton, K. Ip, Y.W. Heo, T. Steiner, Recent progress in processing and properties of ZnO. Prog. Mat. Sci. **50**, 293 (2005)
3. U. Ozgür, Y.I. Alivov, C. Liu, A. Teke, M.A. Reshchikov, S. Doğan, V. Avrutin, S.J. Cho, H. Morkço, A comprehensive review of ZnO materials and devices. J. Appl. Phys. **98**, 041301 (2005)
4. G. Mandel, Self-compensation limited conductivity in binary semiconductors. Phys. Rev. A. **134**, 1037 (1964)
5. C.G. van deWalle, Hydrogen as a cause of doping in Zinc Oxide. Phys. Rev. Lett. **85**, 1012 (2000)
6. C.G. van deWalle, D.B. Laks, C.F. Neumark, S.T. Pantelides, 1st-principles calculations of solubility and doping limits—Li, Na, and N in ZnSe. Phys. Rev. B. **47**, 9425 (1993)
7. D.C. Look, R.L. Jones, J.R. Sizelove, N.Y. Garces, N.C. Giles, L.E. Halliburton, The path to ZnO devices: donor and acceptor dynamics. Phys. Status Solidi A **195**, 171 (2004)
8. K. Minegishi, Y. Koiwai, K. Kikuchi, Growth of p-type Zinc Oxide films by chemical vapor deposition. Jpn. J. Appl. Phys. **36**, L1453 (1997)
9. D.C. Look, D.C. Reynolds, C.W. Litton, R.L. Jones, D.B. Eason, G. Cantwell, Characterization of homoepitaxial p-type ZnO grown by molecular beam epitaxy. Appl. Phys. Lett. **81**, 1830 (2002)
10. K.K. Kim, H.S. Kim, D.K. Hwang, J.H. Lim, S.J. Park, Realization of p-type ZnO thin films via phosphorus doping and thermal activation of the dopant. Appl. Phys. Lett. **83**, 63 (2003)
11. Z.Q. Chen, A. Kawasuso, Y. Xu, H. Naramoto, X.L. Yuan, T. Sekiguchi, R. Suzuki, T. Ohdaira, Production and recovery of defects in phosphorus-implanted ZnO. J. Appl. Phys. **97**, 013528 (2005)
12. Y.R. Ryu, S. Zhu, D.C. Look, J.M. Wrobel, H.M. Jeong, H.W. White, Synthesis of p-type ZnO films. J. Cryst. Growth **216**, 330 (2000)
13. S. Limpijumnong, S.B. Zhang, S.H. Wei, C.H. Park, Doping by large-size-mismatched impurities: The microscopic origin of arsenic- or antimony-doped p-type zinc oxide. Phys. Rev. Lett. **92**, 155504 (2004)
14. B.D. Cullity, Elements of x-ray diffraction, p. 102 (1978)